Sol–gel synthesis of quaternary $(P_2O_5)_{55}$–$(CaO)_{25}$–$(Na_2O)_{(20-x)}$–$(TiO_2)_x$ bioresorbable glasses for bone tissue engineering applications (x = 0, 5, 10, or 15)

Biomedical Materials

PAPER

Sol–gel synthesis of quaternary $(P_2O_5)_{55}$–$(CaO)_{25}$–$(Na_2O)_{(20-x)}$–$(TiO_2)_x$ bioresorbable glasses for bone tissue engineering applications (x = 0, 5, 10, or 15)

Farzad Foroutan[1,2], Nick J Walters[3,4], Gareth J Owens[1], Nicola J Mordan[1], Hae-Won Kim[5,6,7], Nora H de Leeuw[2,8] and Jonathan C Knowles[1,5]

[1] Division of Biomaterials & Tissue Engineering, UCL Eastman Dental Institute, 256 Gray's Inn Road, London WC1X 8LD, UK
[2] Department of Chemistry, University College London, 20 Gordon Street, London WC1H 0AJ, UK
[3] Adult Stem Cell Group, University of Tampere, Finn Medi 5, Biokatu 12, 33014 Tampere, Finland
[4] BioMediTech, Biokatu 10, 33520 Tampere, Finland
[5] Department of Nanobiomedical Science & BK21 Plus NBM Global Research Center for Regenerative Medicine, Dankook University, Cheonan 330–714, Korea
[6] Institute of Tissue Regeneration Engineering & College of Dentistry, Dankook University, Cheonan 330–714, Korea
[7] Department of Nanobiomedical Science Research Centre of Nanobiomedical Science, Dankook University, Chungnam 330–714, Korea
[8] School of Chemistry, Cardiff University, Main Building, Park Place, Cardiff, CF10 3AT, UK

E-mail: j.knowles@ucl.ac.uk

Keywords: sol–gel, phosphate-based glass, bioactive glass, titanium, biomaterial, tissue engineering

OPEN ACCESS

RECEIVED
22 April 2015

REVISED
29 June 2015

ACCEPTED FOR PUBLICATION
23 July 2015

PUBLISHED
26 August 2015

Abstract

In the present study, we report a new and facile sol–gel synthesis of phosphate-based glasses with the general formula of $(P_2O_5)_{55}$–$(CaO)_{25}$–$(Na_2O)_{(20-x)}$–$(TiO_2)_x$, where $x = 0, 5, 10$ or 15, for bone tissue engineering applications. The sol–gel synthesis method allows greater control over glass morphology at relatively low processing temperature (200 °C) in comparison with phosphate-based melt-derived glasses (~1000 °C). The glasses were analyzed using several characterization techniques, including x-ray diffraction (XRD), ^{31}P magic angle spinning nuclear magnetic resonance (^{31}P MAS-NMR), Fourier transform infrared (FTIR) spectroscopy and energy-dispersive x-ray (EDX) spectroscopy, which confirmed the amorphous and glassy nature of the prepared samples. Degradation was assessed by measuring the ion release and pH change of the storage medium. Cytocompatibility was also confirmed by culturing osteoblast-like osteosarcoma cell line MG-63 on the glass microparticles over a seven-day period. Cell attachment to the particles was imaged using scanning electron microscopy (SEM) and confocal laser scanning microscopy (CLSM). The results revealed the potential of phosphate-based sol–gel derived glasses containing 5 or 10 mol% TiO_2, with high surface area, ideal dissolution rate for cell attachment and easily metabolized dissolution products, for bone tissue engineering applications.

1. Introduction

Providing cells with an environment that simultaneously provides a scaffold for regeneration, whilst allowing them to continue their normal functionality is one of the most important issues in tissue engineering. Bioactive and biodegradable materials are favourable due to their ability to break down and stimulate the formation of novel extracellular matrix, and eventually tissue [1, 2]. Phosphate-based glasses are defined as bioresorbable materials with a controllable degradation rate, which makes them an excellent choice for various biomedical applications [3]. These glasses offer an advantageous alternative to silica-based sol–gel derived glasses, with a more controllable degradation rate and easily metabolized dissolution products [4, 5]. The degradation rate, which is typically relatively rapid, can be easily altered via the addition of various modifier oxides, such as calcium oxide (CaO) and sodium oxide (Na_2O) [6]. This enables the design of materials that release Ca^{2+} and Na^+ ions, which can stimulate cellular behaviours such as proliferation and bone formation [4, 7]. The degradation of phosphate-based glasses can also be prolonged by the addition of other oxide elements such as titanium oxide (TiO_2), which forms stable cross-links in the phosphate-network [8]. Glasses of the general formula P_2O_5–CaO–Na_2O–TiO_2

Table 1. Theoretical sol–gel derived glass formulations.

Glass code	Theoretical formulation	Concentration (mol%)			
		P_2O_5	CaO	Na_2O	TiO_2
Ti0	$(P_2O_5)_{55}$–$(CaO)_{25}$–$(Na_2O)_{20}$	55	25	20	0
Ti5	$(P_2O_5)_{55}$–$(CaO)_{25}$–$(Na_2O)_{15}$–$(TiO_2)_5$	55	25	15	5
Ti10	$(P_2O_5)_{55}$–$(CaO)_{25}$–$(Na_2O)_{10}$–$(TiO_2)_{10}$	55	25	10	10
Ti15	$(P_2O_5)_{55}$–$(CaO)_{25}$–$(Na_2O)_5$–$(TiO_2)_{15}$	55	25	5	15

have previously been prepared via the melt-quench method and their biocompatibility and degradation rate extensively studied for a variety of biomedical applications [8, 9]. Few studies exist concerning the preparation of titanium stabilized sol–gel derived phosphate glasses [10, 11], however, and according to the knowledge of the authors, no studies have been published regarding their potential use in tissue regeneration applications. The sol–gel method allows control over glass morphology, which is of fundamental importance in tissue regeneration [12]. In addition, the low processing temperature (200 °C) of the sol–gel synthesis enables the incorporation of bioactive molecules for drug delivery applications. This is not possible with phosphate-based glasses formed by the melt-quench technique, as it requires higher a processing temperature (~1000 °C), and therefore results in degradation of the organic components [8, 10].

The present article reports sol–gel synthesis of novel $(P_2O_5)_{55}$–$(CaO)_{25}$–$(Na_2O)_{(20-x)}$–$(TiO_2)_x$ sol–gel glasses ($x = 0$, 5, 10 or 15) for bone tissue regeneration applications. The structure of the samples was characterized using XRD, ^{31}P MAS-NMR, FTIR, and the elemental proportion was measured using EDX spectroscopy. The pH change of ultrapure water during storage of the sol–gel glass particles at 37 °C was recorded and the release of polyphosphate, calcium and sodium ions was quantified by ion chromatography. Cytocompatibility was also assessed and cells attached to the surface of the glass particles were imaged using SEM and CLSM.

2. Materials and methods

2.1. Materials

The following chemical precursors were used without further purification: *n*-butyl phosphate (1 : 1 molar ratio of mono-*n*-butyl phosphate and di-*n*-butyl phosphate, 98%, Alfa Aesar, Heysham, UK), calcium methoxyethoxide (20% in methoxyethanol, ABCR GmbH, Karlsruhe, Germany), sodium methoxide solution (30 wt% in methanol, Sigma-Aldrich, Gillingham, UK), titanium(IV) isopropoxide (97%, Sigma-Aldrich, Gillingham, UK), 2-methoxyethanol (99.8%, Sigma-Aldrich, Gillingham, UK) and *n*-dimethyl formamide (n-DMF, ⩾ 99.8%, Alfa Aesar, Heysham, UK).

2.2. Methods

2.2.1. Sol–gel synthesis

Sol–gel synthesis was initiated by mixing *n*-butyl phosphate in 2-methoxyethanol at a molar ratio of 1 : 3 for ~10 min in a dry vessel. The reaction was then cooled in an ice bath before the dropwise addition of titanium isopropoxide and calcium methoxyethoxide. Sodium methoxide solution was then added to the mixture and allowed to react for ~1 h. Finally, *n*-DMF was added to the solution at a molar ratio of 0.25 : 1. A total of four glass compositions were synthesized as detailed in table 1. All formulations turned to gel within 5 min at room temperature. Samples were aged for 3 d, before the temperature was gradually increased to 60 °C and maintained for 7 d. Following that, the temperature was increased to 120 °C for 4 d and then 180 °C for 2 d, before a final drying stage at 200 °C for 2 h to evaporate any remaining solvent. The obtained sol–gel glasses were ground at 10 Hz to form microparticles (MM301 milling machine, Retsch GmbH, Hope, UK). Microparticles in the size range of 106–150 μm were obtained using test sieves (Endecotts Ltd, London, UK) and a sieve shaker (Spartan, Fritsch GmbH, Brackley, UK).

2.2.2. Materials characterization

2.2.2.1. EDX EDX (Inca 300, Oxford Instruments, Abingdon, UK) was used to determine the exact compositions of the prepared samples. SEM (XL30, Philips, Eindhoven, Netherlands) was operated at 20 kV, spot size 5 and a working distance of 10 mm, in order to identify the particular elements and their relative proportions with EDX from the scanned area.

2.2.2.2. XRD XRD (D8 Advance Diffractometer, Brüker, Coventry, UK) was performed on samples in a flat plate geometry using Ni filtered Cu Kα radiation, in order to determine crystallinity. Data were collected using a Lynx Eye detector with a step size of 0.02° over an angular range of $2\theta = 10$–100° and a count time of 12 s.

2.2.2.3. ^{31}P MAS-NMR A ^{31}P spectrum of each glass composition was acquired by magic angle spinning solid-state nuclear magnetic resonance (VNMRS-400 Spectrometer, Varian, Crawley, UK) and referenced to the resonance of the secondary reference ammonium dihydrogen phosphate ($NH_4H_2PO_4$) at 0.9 ppm (relative to 85% H_3PO_4 solution at 0 ppm). The spectra

were recorded at 161.87 MHz, for which samples were loaded into a 4 mm (rotor o.d.) magic angle-spinning probe. Spectra were obtained using direct excitation with a 90° pulse and 60 s recycle delay at ambient probe temperature (~25 °C) and at a sample spin rate of 10 kHz. Between 20 and 88 repetitions were accumulated for each composition and were processed using Dm-fit software [13].

2.2.2.4. FTIR An FTIR spectrum of each glass composition was acquired (FT-IR 2000 and Timebase software, Perkin Elmer, Seer Green, UK) with an attenuated total reflectance accessory (Golden Gate, Specac, Orpington, UK). Solid glass powder was scanned at room temperature in absorbance mode in the range of 1600–600 cm^{-1}.

2.2.3. Glass degradation

In order to measure the ion release and pH changes, glass degradation was assessed in ultrapure water. Alternative storage media include solutions such as simulated body fluid (SBF), cell culture medium and Tris-HCl. The ions being measured, however, occur at high concentrations in SBF and cell culture medium and therefore mask the relatively low levels of ions released from the sol–gel derived glasses. In addition, the SBF and cell culture medium act as a buffering agent that does not allow accurate measurement of the pH changes. Furthermore, Tris-HCl can interfere with the ion chromatography column, hence the use of ultrapure water.

2.2.3.1. pH change Specimens of each composition (25 mg, $n = 3$) were immersed in 5.5 ml ultrapure water (pH 7.0 ± 0.1) and stored at 37 °C for up to 7 d. The pH of the water was measured after 0, 1, 3 and 7 d (Orion pH Meter, Thermo Scientific-Orion Star, UK). At each time-point, the particles were centrifuged at 4000 rpm for 10 min, in order to separate them from the solution. The supernatant was aspirated and the particles dried in an oven at 60 °C for 3 h, before replenishment with fresh ultrapure water.

2.2.3.2. Ion release Specimens of each composition (50 mg, $n = 3$) were immersed in 11 ml ultrapure water (pH 7.0 ± 0.1) and stored at 37 °C for up to 7 d. The release of cations (Na^+ and Ca^{2+}) and anions (PO_4^{3-}, $P_2O_7^{4-}$, $P_3O_9^{3-}$, and $P_3O_{10}^{5-}$) was quantified after 0, 1, 3 and 7 d using ion chromatography, as previously described [14]. At each time-point, glass suspensions were centrifuged at 4000 rpm for 20 min, in order to separate them from the solution. The supernatant was collected and the particles dried in an oven at 60 °C for 3 h, before replenishment with fresh ultrapure water. Liquid samples were passed through OnGaurd IIA filters (Dionex, Thermo Scientific, Hemel Hempstead, UK) before cation analysis using an ICS-1000 system (Dionex) equipped with a CS12A column operating under suppressed conductivity, with 20mM methanesulfonic acid eluent. Anions were measured using an ICS-2500 system (Dionex) equipped with an AS16 column operating under suppressed conductivity. Isocratic separation was applied with a linear KOH gradient of between 30–50mM over a 35 min period provided by an EG50 eluent generator. Data analyses were performed in relation to standard solutions using Chromelon software (Dionex). The results were extrapolated from standard curves, prepared from standard solutions provided by the manufacturer (Dionex).

2.2.4. Cell studies

2.2.4.1. Cell culture Human osteoblast-like osteosarcoma cell line (MG-63, European Collection of Cell Cultures, Porton Down, UK) was cultured under standard conditions (37 °C, 95% air, 5% CO_2, 95% relative humidity) in Dulbecco's modified Eagle medium (DMEM, Gibco, Life Technologies, Paisley, UK) supplemented with 10% foetal bovine serum (Gibco).

2.2.4.2. Cytocompatibility assay In order to assess the effect of TiO_2 content of the sol–gels on cytocompatibility, MG-63 cells were cultured on the microparticles. The materials were sterilized by dry heat during sample preparation. The sol–gel particles (5 mg per specimen) were evenly distributed across permeable cell culture supports in 48 well plates (Transwell, Corning B.V. Lifesciences, Amsterdam, Netherlands), in order to enable facile processing of the specimens for SEM and confocal microscopy after the final time-point. Cells were seeded on the particles at a density of 30 000 cells cm^{-2} (10 000 cells/well) and the cell culture medium was added to the cell culture support and the bulk of the well (1.1 ml total). Controls consisted of cells seeded directly on cell culture supports. Each sample type was analyzed in triplicate. Cytocompatbility was assessed after 1, 3 and 7 d. At each time-point, cells were seeded at various densities, 2 h prior to the assay, for the preparation of standard curves. The medium was then aspirated from the samples and standards and replaced with 1 ml medium containing 10 vol% water soluble tetrazolium salt-8 (WST-8, Cell Counting Kit-8, Sigma Aldrich, Gillingham, UK). WST-8 is a pink substrate, which is metabolized in the mitochondria to form an orange formazan product. After 80 min incubation at 37 °C, absorbance at 460 nm (with a reference wavelength of 650 nm) was measured (Infinite M200, Tecan, Männedorf, Switzerland). The apparent cell density of the samples was extrapolated from the standard curves. The WST-8-containing medium was then aspirated and replaced with a fresh cell culture medium until the next time-point. Following the final time-point, the cells residing on the microparticles were imaged by CLSM and SEM.

2.2.4.3. Cell and particle imaging Specimens consisting of MG-63 cells cultured on the sol–gel

Table 2. Measured compositions of sol–gel derived glasses, determined by EDX.

Glass code	Concentration (mol%)			
	P_2O_5	CaO	Na_2O	TiO_2
Ti0	47.0 (±1.0)	30.8 (±0.8)	22.2 (±0.6)	—
Ti5	49.6 (±1.0)	27.2 (±0.7)	16.3 (±0.6)	6.9 (±0.5)
Ti10	50.2 (±1.0)	26.9 (±0.8)	11.7 (±0.6)	11.2 (±0.5)
Ti15	50.9 (±1.1)	26.5 (±0.6)	6.1 (±0.5)	16.5 (±0.7)

microparticles for 7 d were prepared by fixation in 3% glutaraldehyde, followed by dehydration through a graded series of ethanols (50%, 70%, 90% and 100%) and drying in hexamethyldisilazane (Sigma-Aldrich). This was carried out *in situ* in the cell culture supports, after which the membranes were carefully excised using a scalpel and mounted on aluminium stubs using araldite. The specimens were then sputter-coated with gold/palladium alloy and imaged using SEM, with an accelerating voltage of 5 kV and working distance of 10 mm.

Cells residing on sol–gel microparticles were imaged using CLSM after 7 d culture. The cytoskeleton (actin filaments) and nuclei of the cells were fluorescently stained using Alexa Flour 488 phalloidin and propidium iodide, respectively. Specimens were prepared by fixation in 4% paraformaldehyde, followed by two washes using Dulbecco's phosphate buffered saline (D-PBS, Lonza, Slough, UK). Cells were then permeabilized using a 0.1% solution of Triton X-100 (Sigma-Aldrich) in D-PBS for 5–10 min at room temperature. A 2.5% solution of phalloidin methanolic stock solution (Invitrogen) in D-PBS was then added to each specimen and incubated for 20 min at room temperature in a dark environment, in order to minimize evaporation and photo-bleaching. After a further two washes with D-PBS, the specimens were counter-stained using 1 μg ml^{-1} propidium iodide (BD Biosciences, Oxford, UK) for 10 min, before visualization by CLSM (Biorad, Hemel Hempstead, UK).

3. Results

3.1. Material properties

3.1.1. EDX

The measured compositions of sol–gel glasses, as determined by EDX, are presented in table 2. Ti0 showed the highest reduction of P_2O_5 content (8 mol%), with a gradual increase correlated with substituting sodium for titanium up to 4.1 mol% reduction (Ti15) compared to the theoretical value. This was compensated by a concomitant increase in the content of other oxides (CaO, Na_2O and TiO_2).

3.1.2. XRD

Figure 1 shows the XRD spectra of sol–gel derived specimens. In all the compositions, a broad peak at 2θ values between 20° and 40° was observed and was free from any detectable crystalline phase, confirming the amorphous nature of the sol–gel derived glasses.

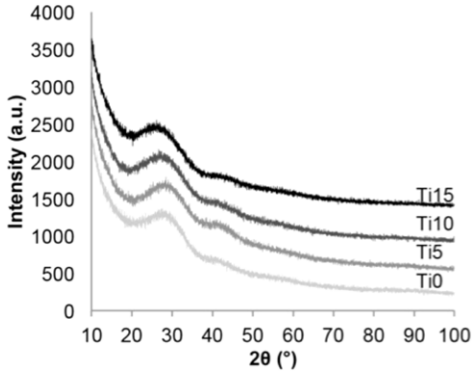

Figure 1. XRD spectra of sol–gel derived glasses containing 0, 5, 10 or 15 mol% TiO_2. No crystalline phase was detectable, indicating the amorphous nature of the sol–gel derived glasses.

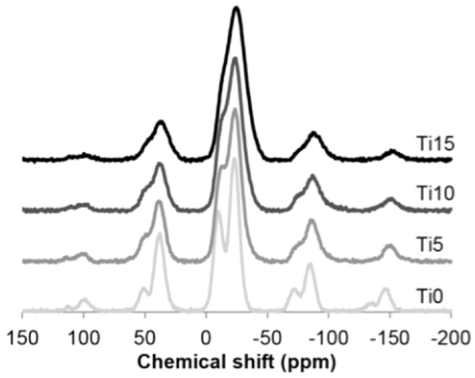

Figure 2. ^{31}P MAS-NMR spectra of sol–gel derived glasses containing 0, 5, 10 or 15 mol% TiO_2, representing the number of bridging oxygen atoms in the PO_4^{3-} group connected to other such phosphate tetrahedra to form a network.

Table 3. ^{31}P MAS-NMR peak parameters of sol–gel derived glasses.

Glass code	Position (ppm,±0.2)	Q^i species	Line width (ppm, ± 0.2)	Abundance (%, ±1.0)
Ti0	− 9.9	1	8.3	30.4
	− 23.1	2	9.4	69.6
Ti5	− 9.9	1	8.5	21.3
	− 13.6	1	8.3	4.3
	− 23.2	2	12.4	74.4
Ti10	− 10.1	1	8.9	12.5
	− 14.0	1	8.4	7.9
	− 23.2	2	13.1	79.6
Ti15	− 10.3	1	9.4	6.1
	− 14.1	1	9.6	9.7
	− 23.8	2	13.6	84.2

3.1.3. ^{31}P MAS-NMR

The ^{31}P MAS-NMR spectra of the sol–gel derived glasses are displayed in figure 2 and the peak parameters are summarized in table 3. The resonances in the ^{31}P MAS-

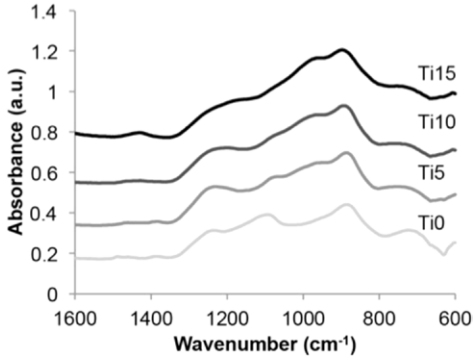

Figure 3. FTIR spectra of sol–gel derived glasses containing 0, 5, 10 or 15 mol% TiO_2. Different peak positions were correlated with various Q^n phosphate units ($n = 1$ or 2).

Table 4. Infrared band assignment for sol–gel derived glasses.

Wavenumber (cm^{-1})	Assignments	Associated Q^i
730	υ_s (P–O–P)	N/A
900	υ_{as} (P–O–P)	Q^2
970	υ_s $(PO_3)^{2-}$	Q^1
1100	υ_{as} $(PO_3)^{2-}$	Q^1
1235	υ_{as} (PO_2)	Q^2

Note: υ, stretching; $_s$, symmetric; $_{as}$, asymmetric.

NMR spectra are assigned to various Q^n species, where n represents the number of bridging oxygen atoms in the PO_4^{3-} group that are connected to another such phosphate tetrahedron to form a network [15, 16]. Peaks in the range of −9.9 to −10.3 ppm are attributed to Q^1 phosphate units, while peaks in the range of −13.6 to −14.1 ppm and −23.1 to −23.8 ppm correspond to the Q^1 (Ti–O–P) and Q^2 species, respectively [10, 17, 18].

3.1.4. FTIR

The FTIR spectra of the sol–gel glasses are presented in figure 3. Table 4 shows the infrared band assignment. The peaks at 900 and 1235 cm^{-1} can be assigned to the Q^2 phosphate units, while the peaks at 970 and 1100 cm^{-1} can be related to the Q^1 phosphate units [19]. Increases in the intensity of the peaks at 900 cm^{-1} were correlated with the increasing substitution of sodium with titanium.

3.1.5. Glass degradation

The pH of the dissolution products of all the compositions underwent a notable reduction over the first 24 h, as shown in figure 4. A more gradual decrease in pH progressed during the remainder of the immersion period. Increasing TiO_2 content in the sol–gel derived glasses reduced the extent and rate of the pH decrease, although there was little difference between Ti5, Ti10 and Ti15.

Figures 5 and 6 illustrate the release of cations (Ca^{2+} and Na^+) and anions ($P_2O_7^{4-}$, $P_3O_{10}^{5-}$, $P_3O_9^{3-}$ and PO_4^{3-}) from the sol–gel glass particles, respectively. As expected, higher concentrations of Ca^{2+} were detected

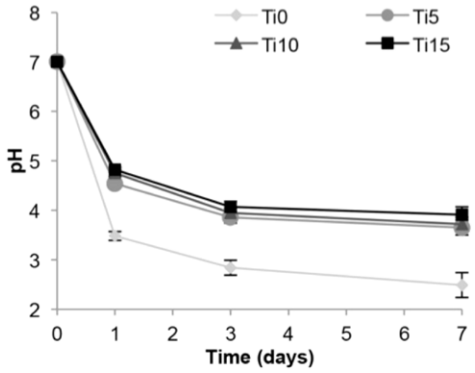

Figure 4. pH measurement after 0, 1, 3 and 7 d immersion of sol–gel derived glass particles in deionized water. The pH decreased significantly after 24 h, followed by a more gradual decrease. Increasing the TiO_2 content reduced the extent and rate of the pH change.

in samples collected from glasses with lower TiO_2 content. Likewise, the Na^+ release showed a clear distinction between each glass composition. Glasses with lower Na_2O content released less Na^+ into the solution. The release of Ti^{4+} was also investigated but was below the detectable range.

Similarly, the release of the $P_2O_7^{4-}$ and $P_3O_{10}^{5-}$ anions correlated directly with the TiO_2 content, with an increasing Ti resulting in a decreasing release. The $P_3O_9^{3-}$ and PO_4^{3-} release, however, followed trends that were distinct from a direct relationship with the Ti content. Ti5 and Ti10 demonstrated a higher $P_3O_9^{3-}$ release than Ti0 and Ti15. Conversely, the release of PO_4^{3-} from Ti0 and Ti5 was markedly lower than from Ti10 and Ti15.

3.1.6. Cytocompatibility

The cytocompatibility of the sol–gel derived glasses is presented in figure 7. The control (MG-63 on cell culture supports) approximately doubled in apparent cell density at each time-point, reaching 217 000 cells cm^{-2} by day 7. The apparent density of the cells cultured on glass particles remained low after 1 and 3 d. Ti0 caused the cells to approximately halve in number within the first day, with little subsequent recovery. A concurrent increase in acidity was noted in Ti0, as the phenol red in the cell culture medium turned from pink to a light orange colour. The cells cultured on Ti5 and Ti10 had a low apparent cell density after 1 and 3 d, but this recovered to 135 000 and 212 000 cells cm^{-2} by day 7, respectively. Ti15, however, had poor cytocompatibility, with cells failing to recover even after 7 d.

3.1.7. Cell and particle imaging

The morphology and size of the sol–gel particles was identified by SEM (figure 8) after 7 d in the cell culture. All the compositions had a similar morphology, with particles assuming a jagged but generally spherical form, with diameters in the range of ~0.5–2 μm and a rough surface topography. The control (a), (b) shows a monolayer of cells spread on the cell culture support (dark circular features are pores). After 7

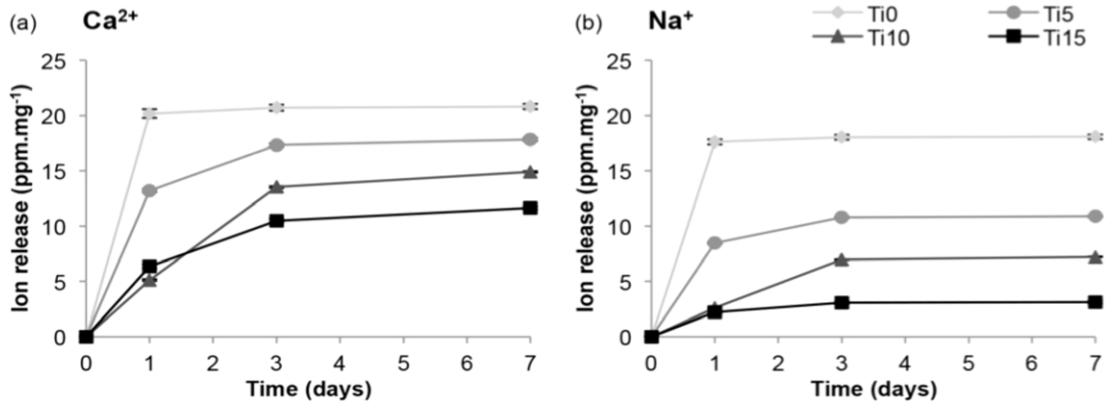

Figure 5. Cumulative release of (a) Ca^{2+} and (b) Na^{+} cations from sol–gel derived glass particles after 1, 3 and 7 d storage in ultrapure water. Decreasing the release of Ca^{2+} and Na^{+} was associated with increasing the substitution of Na with Ti. Error bars are SD ($n = 3$).

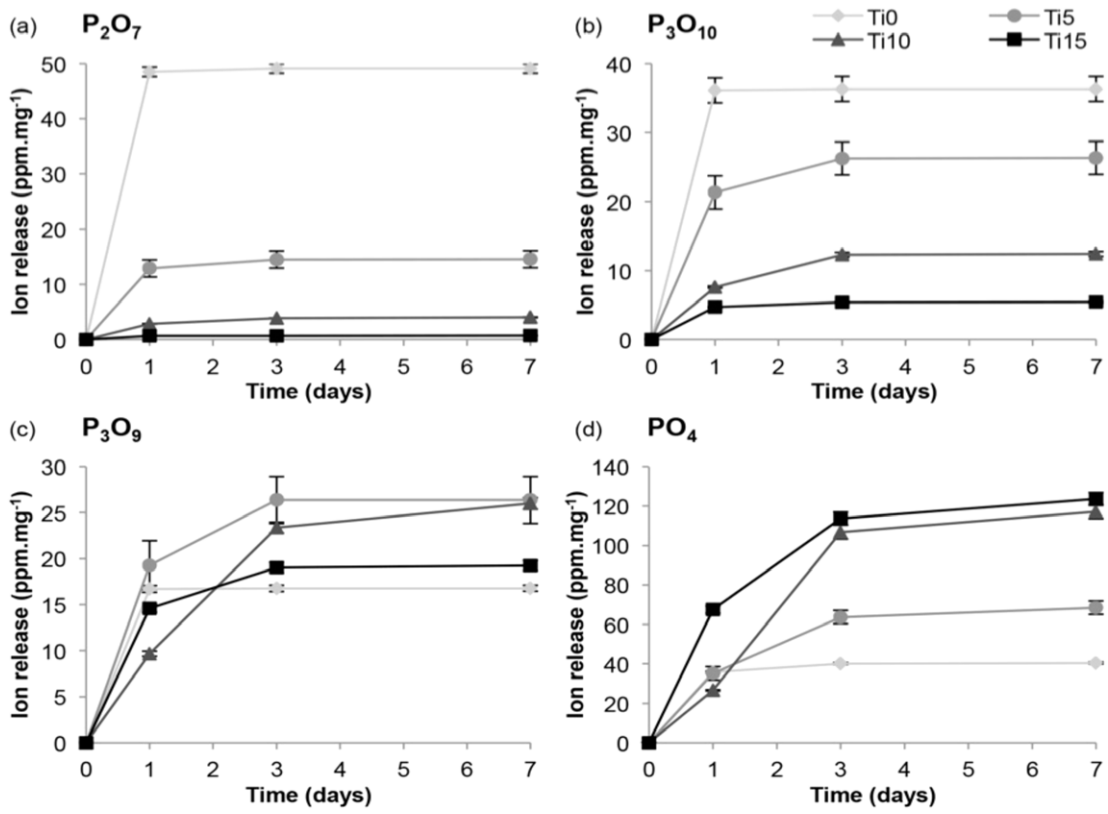

Figure 6. Cumulative release of (a) $P_2O_7^{4-}$, (b) $P_3O_{10}^{5-}$, (c) $P_3O_9^{3-}$ and (d) PO_4^{3-} anions from sol–gel derived glass particles after 1, 3 and 7 d storage in ultrapure water. Decreasing the release of $P_2O_7^{4-}$ and $P_3O_{10}^{5-}$ was associated with increasing the substitution of Na with Ti. The release of PO_4^{3-} from Ti10 and Ti15 was approximately double that from Ti0 and Ti5. Ti5 and Ti10 released significantly more $P_3O_9^{3-}$ than Ti0 and Ti15. Error bars are SD ($n = 3$).

d in the culture, the Ti0 particles (c), (d) had almost fully degraded and therefore the cells could not be visualized on the remaining small particles or on the surface of the cell culture insert. Some cells were visible on the surface of Ti5 particles (e), (f), although this was much more apparent on the surface of Ti10 (g)–(j). At high magnification the cells can be observed to have stretched and formed a flattened morphology on the surface of a Ti10 particle (i), (j). The Ti10 and Ti15 particles remained large, suggesting minimal degradation, although no cells were visible on Ti15 (k), (l). Figure 9 shows CLSM images of the cells attached to the Ti5 and Ti10 microparticles. Cells were not observed on Ti0 or Ti15.

4. Discussion

In the present study, phosphate-based glasses with the general formula of P_2O_5–CaO–Na_2O and P_2O_5–CaO–Na_2O–TiO_2 were successfully synthesized via the sol–gel method for bone tissue engineering applications. The XRD spectra confirmed the amorphous and glassy

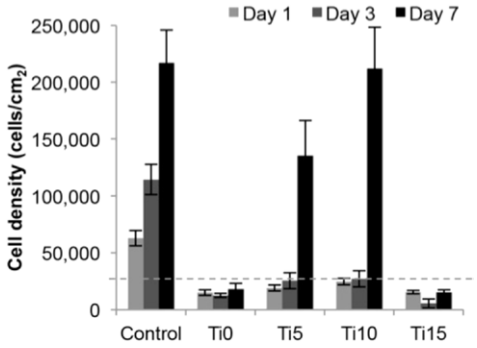

Figure 7. Cytocompatibility of sol–gel derived glass micrscopheres containing 0, 5, 10 or 15 mol% Ti with MG-63 at 1, 3 and 7 d. Ti5 and particularly Ti10 had good cytocompatibility, whereas Ti0 and Ti15 had poor cytocompatibility. The dotted line represents the initial seeding density. Error bars are SD ($n = 3$).

nature of all glass compositions and EDX revealed a relatively low loss of phosphorus (up to 8 mol%), which was due to the evaporation of the unreacted phosphorus precursor within the sol–gel reaction. Interestingly, substituting sodium for titanium reduced the phosphorus loss to around 4 mol%. This was due to the cross-linking effect of titanium that increased the polymerization of the phosphate network [10, 20]. The cross-linking effect was investigated by ^{31}P MAS-NMR and FTIR. These spectra showed the formation of Q^1 (Ti–O–P) and also confirmed an increase in Q^2 species.

The sol–gel derived glass particles were immersed in ultrapure water for 0, 1, 3 and 7 d and their degradation was analyzed by ion chromatography and by measuring the pH change of the water. Ion chromatography was favoured over inductively coupled plasma spectroscopy due to its ability to differentiate between different phosphate species. This is particularly important when studying the dissolution of glasses in which phosphate is a major component. Tris-HCl was not used, due to the presence of organic solvents which irreversibly bind to the ion chromatography column. Since simulated body fluid is super-saturated with the same ions being released from the glasses, it was also selected against, as the concentration of released ions would have been difficult to distinguish from the high background levels. A clear initial decrease in pH was observed within 24 h for all compositions, followed by a more gradual decrease at later time-points. This suggested that increasing the TiO_2 content reduced the rate of pH reduction, since titanium has a high charge/diameter ratio that can make the phosphate network more interconnected. As expected, higher calcium release was associated with lower titanium content. Likewise, the release of sodium followed a similar pattern, which can be explained on the basis of substitution between sodium and titanium within the present glass compositions. A similar trend was observed for $P_2O_7^{4-}$ and $P_3O_{10}^{5-}$.

The detected levels of $P_3O_9^{3-}$ and PO_4^{3-} follow more complex trends. As the $P_3O_9^{3-}$ release reached a maximum for Ti0, which was below that of the other compositions, this may reflect that the entire $P_3O_9^{3-}$ content of the glass had been released into the solution. $P_3O_9^{3-}$ is a cyclic molecule composed of three phosphate units. In order to form, it can be reasoned that phosphate alkoxides would need to be in close proximity to each other at the point of synthesis without other network forming units. With the higher valency of Ti increasing network connectivity in comparison to Na, the number of phosphate bonds that form with other phosphate units is expected to be reduced by increasing Ti [21]. Hence, a lower degree of $P_3O_9^{3-}$ would be present within the Ti0 glass. PO_4^{3-} may also be released as a result of smaller phosphate units within the glass network. It should also be noted, however, that linear molecules lack the stability of cyclic structures. Taking this into consideration, variable trends in PO_4^{3-} release are to be reasonably expected, as the PO_4^{3-} detected in solution thus represents the accumulation of PO_4^{3-} released directly from the glass and PO_4^{3-} formed by the degradation of longer chain polyphosphates in solution. These results are also corroborated by the initial pH data collected. For example, highly acidic species such as $P_2O_7^{4-}$ and $P_3O_{10}^{5-}$ were released in the greatest amount from the Ti0 glass and this particular composition also induced the greatest pH reduction in solution [22]. Likewise, less acidic PO_4^{3-} and $P_3O_9^{3-}$ species were released in proportionally greater amounts from those glasses which reduced the pH of the solution to a lesser extent [23].

The apparent cell density of MG-63 cells cultured on a layer of sol–gel derived glass particles was reduced in comparison to the cell culture support control after 1 and 3 d in the case of all the compositions. This was likely caused by the rapid decrease in pH that occurred upon glass degradation. Although the pH change would have been partially buffered by the cell culture medium, the more extreme drop in pH in Ti0 explains why the cells failed to recover and reach initial seeding density. As the Ti content was increased from 0 to 5 or 10 mol%, the density of the surviving cells increased in parallel, due to the decrease in glass degradation and lower drop in pH. The apparent density of cells residing on Ti5 after 7 d in culture had recovered to ~60% that of the control, whereas cells cultured on Ti10 had recovered to the same level as the control. Cells cultured on Ti15, however, failed to recover. No cells were visible in the SEM or CLSM images and only low cell densities were detected by WST-8.

Furthermore, of the anions investigated, only PO_4^{3-} contributes to apatite formation, whereas longer chain polyphosphates are known to inhibit crystal growth [24]. As apatite formation is believed to promote cellular attachment [25], the deposition of a mineral layer at the interface of the glass and its environment is a plausible explanation of the high cytocompatibility of Ti10. The reduced survival of cells cultured on Ti15, however, requires further explanation. Titanium has been shown to inhibit hydroxyapatite mineralization and may pre-

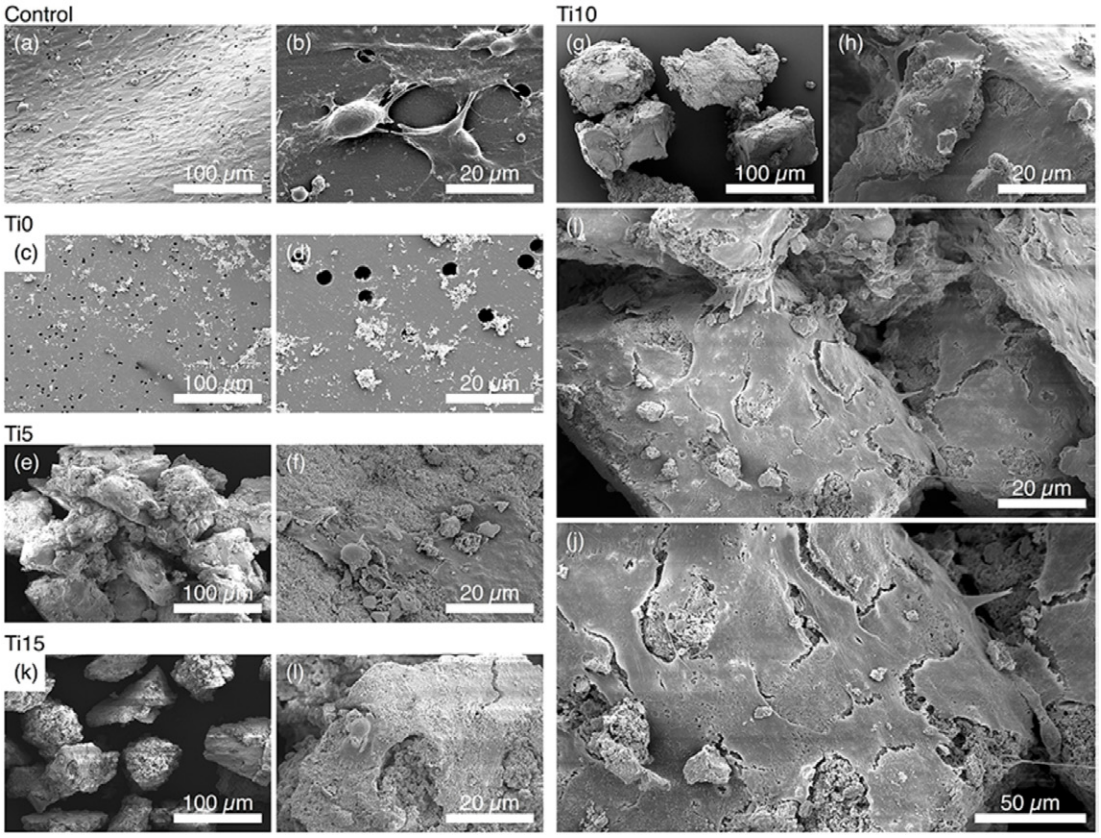

Figure 8. Scanning electron micrographs showing particle size and morphology and cell attachment. (a), (b) Control (cells on cell culture support), (c), (d) Ti0, (e), (f) Ti5, (g)–(j) Ti10 and (k), (l) Ti15. Cells were observed on the surfaces of Ti5 and Ti10 but not Ti0, which had largely dissolved, or Ti15, which was intact.

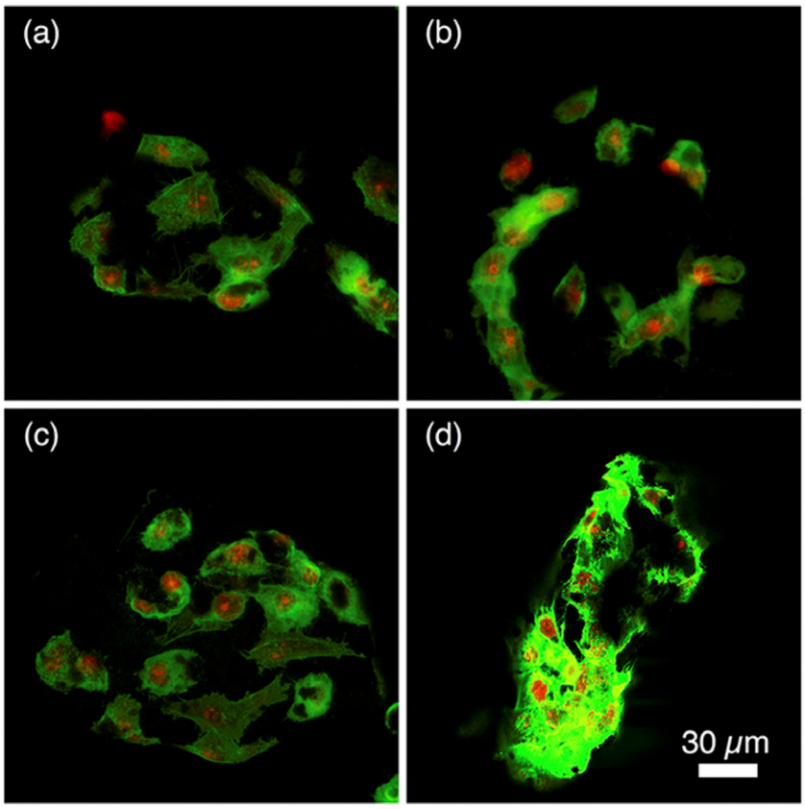

Figure 9. Confocal micrographs showing cells attached to sol–gel derived glass microparticles containing (a), (b) 5 or (c), (d) 10 mol% Ti. The green fluorescent stain (phalloidin) shows filamentous actin and the red one (propidium iodide) shows nuclei. Scale bar in (a), (b), (c) and (d) is 30 μm.

vent the formation of a hydroxyapatite surface layer amenable to cellular growth [26]. The other possibility may be related to the greater retention of toxic residual solvents by the more highly cross-linked composition. This possible explanation is beyond the scope of this study and would require further investigation.

Furthermore, it is worth noting that water-soluble cell proliferation assays such as WST-8 measure mitochondrial metabolic activity and only give an indication of cell density. It is possible that the lower readings after 1 and 3 d may have been due to lower metabolic activity as the cells attached to the unfamiliar particles and spread across their surface. This would explain the large difference in apparent cell densities between days 3 and 7. It is also possible that the layer of sol–gel glasses on the cell culture support somewhat inhibited the diffusion of nutrients across the membrane, compared to the control.

These results were also supported by the SEM and CLSM images, which showed cells residing on Ti5 and Ti10 but not Ti0 or Ti15. Furthermore, the scanning electron micrographs clearly showed notable mineral formation on the surface of Ti5 and Ti10. Since bone cells strongly favour rough surface topographies for adhesion and proliferation [27], the mineral content and morphology of these compositions provide a possible explanation of their improved cytocompatibility. Although it was beyond the scope of the present research, further studies into the effects of glass composition on alkaline phosphatase activity and gene expression could elucidate the effects of ion release, topographical features and wettability on bone formation.

Finally, it should be noted that sol–gel glass microparticles have a significantly larger surface area than discs composed of melt-quench glass. A recent study of melt-quench glasses with similar compositions to those assessed here, containing 0, 5, 10 or 15 mol% TiO_2, showed significantly higher relative growth of human osteosarcoma cells on discs containing $\geqslant$5 mol% TiO_2 than on those lacking Ti at all time-points studied [28]. In the present research, microparticles containing 5 or 10 mol% TiO_2 supported more efficient cell proliferation after 7 d than those without Ti. Although the sol–gel glasses containing 5 or 10 mol% TiO_2 were shown to have a low degradation rate, their degradation was likely more rapid than the melt-quench glasses of similar compositions, due to their surface area being several orders of magnitude higher. This is the most likely explanation for why the cells on the sol–gel glass microparticles took longer to proliferate than those on the melt-quench glass discs. The biological performance of these microparticles when used in tissue engineering applications such as coatings, however, would likely be improved compared to the present *in vitro* results, since they would be formed into a thinner, more dense and homogenous layer than was studied.

Future work will be focused on developing these materials for technological purposes, such as coatings on various substrates for biomedical applications. Thin or thick films can be made by spray, spin and dip coating on medical implants. In addition, the low processing temperature of the sol–gel synthesis enables the incorporation of bioactive molecules that can promote bone formation, or antimicrobial drugs to be subsequently released in a localized and controlled manner.

5. Conclusions

In this study, quaternary phosphate-based glasses containing up to 15 mol% TiO_2 were successfully synthesized via a facile sol–gel method at relatively low processing temperature for bone tissue engineering applications. The high surface area, controllable dissolution rate and easily metabolized dissolution products of the titanium-stabilized phosphate based sol–gel derived glasses had a considerable effect on cell adhesion, growth and proliferation. The substitution of Na_2O with 5 or 10 mol% TiO_2 reduced the dissolution rate and improved cytocompatibility. The resulting materials have potential applications in medical implant coatings.

Acknowledgments

This project was supported by the UCL Industrial Doctorate Centre in Molecular Modelling & Material Science and in part (JCK & HWK) by National Research Centers Program (2009-0093829) through the National Research Foundation (NRF), Republic of Korea. The authors are grateful to Dr David Apperley for performing ^{31}P MAS-NMR measurements (EPSRC NMR Service, Department of Chemistry, Durham University).

References

[1] Langer R and Vacanti J P 1993 Tissue engineering *Science* **260** 920–6
[2] Hench L L and Polak J M 2002 Third-generation biomedical materials *Science* **295** 1014–7
[3] Knowles J C 2003 Phosphate based glasses for biomedical applications *J. Mater. Chem.* **13** 2395–401
[4] Navarro M, Ginebra M P and Planell J A 2003 Cellular response to calcium phosphate glasses with controlled solubility *J. Biomed. Mater. Res.* A **67A** 1009–15
[5] Hamadouche M 2001 Long-term *in vivo* bioactivity and degradability of bulk sol–gel bioactive glasses *J. Biomed. Mater. Res.* **54** 560–6
[6] Franks K, Abrahams I and Knowles J C 2000 Development of soluble glasses for biomedical use: I. *In vitro* solubility measurement *J. Mater. Sci., Mater. Med.* **11** 609–14
[7] Salih V, Franks K, James M, Hastings G W, Knowles J C and Olsen I 2000 Development of soluble glasses for biomedical use: II. The biological response of human osteoblast cell lines to phosphate-based soluble glasses *J. Mater. Sci., Mater. Med.* **11** 615–20
[8] Kiani A *et al* 2012 Titanium-containing bioactive phosphate glasses *Phil. Trans. R. Soc.* A **370** 1352–75
[9] Lakhkar N J *et al* 2012 Titanium phosphate glass microspheres for bone tissue engineering *Acta Biomater.* **8** 4181–90
[10] Foroutan F *et al* 2015 Novel sol–gel preparation of $(P_2O_5)_{0.4}$ $-(CaO)_{0.25}-(Na2O)_X-(TiO_2)_{0.35-X}$ bioresorbable glasses ($X = 0.05, 0.1$, and 0.15) *J. Sol–Gel Sci. Technol.* **73** 434–42

[11] Pickup D M, Wetherall K M, Knowles J C, Smith M E and Newport R J 2008 Sol–gel preparation and high-energy XRD study of $(CaO)_x(TiO_2)_{0.5-x}(P_2O_5)_{0.5}$ glasses ($x = 0$ and 0.25) *J. Mater. Sci., Mater. Med.* **19** 1661–8
[12] Hench L L 1997 Sol–gel materials for bioceramic applications *Curr. Opin. Solid State Mater.* **2** 604–10
[13] Massiot D *et al* 2002 Modelling one- and two-dimensional solid-state NMR spectra *Magn. Reson. Chem.* **40** 70–6
[14] Abou Neel E A, Chrzanowski W and Knowles J C 2008 Effect of increasing titanium dioxide content on bulk and surface properties of phosphate-based glasses *Acta Biomater.* **4** 523–34
[15] Brow R K 2000 Review: the structure of simple phosphate glasses *J. Non-Cryst. Solids* **263** 1–28
[16] Kirkpatrick R J and Brow R K 1995 Nuclear-magnetic-resonance investigation of the structures of phosphate and phosphate-containing glasses—a review *Solid State Nucl. Magn. Reson.* **5** 9–21
[17] Lee I H, Foroutan F, Lakhkar N J, Gong M S and Knowles J C 2013 Sol–gel synthesis and structural characterization of P_2O_5–CaO–Na_2O glasses *Phys. Chem. Glasses—Eur. J. Glass Sci. Technol.* B **54** 115–20
[18] Montagne L, Daviero S, Palavit G. Glass network evolution with Bi^{3+}/Ti^{4+} substitution in phosphate glasses formulated with a constant oxygen/phosphorus ratio. EXAFS, XANES, and P-31 double quantum MAS NMR *Chem. Mater.* **15** 4709–16
[19] Pickup D M, Guerry P, Moss R M, Knowles J C, Smith M E and Newport R J 2007 New sol–gel synthesis of a $(CaO)_{0.3}(Na_2O)_{0.2}(P_2O_5)_{0.5}$ bioresorbable glass and its structural characterisation *J. Mater. Chem.* **17** 4777–84
[20] Brauer D S, Karpukhina N, Law R V and Hill R G 2010 Effect of TiO_2 addition on structure, solubility and crystallisation of phosphate invert glasses for biomedical applications *J. Non-Cryst. Solids* **356** 2626–33
[21] Pickup D M *et al* 2008 TiK-edge XANES study of the local environment of titanium in bioresorbable TiO_2–CaO–Na_2O –P_2O_5 glasses *J. Mater. Sci., Mater. Med.* **19** 1681–5
[22] Montchamp J L 2015 *Phosphorus Chemistry I: Asymmetric Synthesis and Bioactive Compounds* (Cham: Springer)
[23] Fluck E 1978 *Phosphor Phosphorus. An Outline of its Chemistry, Biochemistry and Technology* ed D E C Von Corbridge (Amsterdam: Elsevier) vol 26 p 386
[24] Driessens F C M 1982 *Mineral Aspects of Dentistry (Monographs in Oral Science)* (Basel: Karger) p 10
[25] Hu H J, Qiao Y Q, Meng F H, Liu X Y and Ding C X 2013 Enhanced apatite-forming ability and cytocompatibility of porous and nanostructured $TiO_2/CaSiO_3$ coating on titanium *Colloid Surf.* B **101** 83–90
[26] Blumenthal N C and Cosma V 1989 Inhibition of apatite formation by titanium and vanadium ions *J. Biomed. Mater. Res.* A **23** 13–22
[27] Walters N J and Gentleman E 2015 Evolving insights in cell–matrix interactions: Elucidating how non-soluble properties of the extracellular niche direct stem cell fate *Acta Biomater.* **11** 3–16
[28] Abou Neel E A, Chrzanowski W and Knowles J C 2014 Biological performance of titania containing phosphate-based glasses for bone tissue engineering applications *Mater. Sci. Eng.* C **35** 307–13